EARTH SURFACE PROCESSES AND LANDFORMS
*Earth Surf. Process. Landforms* **34**, 867–881 (2009)

Published online 4 March 2009 in Wiley InterScience
(www.interscience.wiley.com) DOI: 10.1002/esp.1794

# Parameterizing a physically based shallow landslide model in a data poor region

**Sekhar L. Kuriakose,[1]* L. P. H. van Beek[2] and C. J. van Westen[1]**
[1] International Institute for Geo-information Science and Earth Observation (ITC), Enschede, The Netherlands
[2] Department of Physical Geography, Utrecht University, Utrecht, The Netherlands

Received 15 January 2008; Revised 30 November 2008; Accepted 12 December 2008

* Correspondence to: Sekhar Lukose Kuriakose, United Nations University-ITC School for Disaster Geo-information Management, International Institute for Geo-information Science and Earth Observation (ITC), Hengelosestraat 99, P.O. Box 6, 7500AA, Enschede, The Netherlands. E-mail: sekhar.lk@gmail.com

Earth Surface Processes and Landforms

ABSTRACT: Shallow landslides and consequent debris flows are an increasing concern in the Western Ghats of Kerala, India. Their increased frequency has been associated with deforestation and unfavourable land-use practices in cultivated areas. In order to evaluate the influence of vegetation on shallow slope failures a physically based, dynamic and distributed hydrological model (STARWARS) coupled with a probabilistic slope stability model (PROBSTAB) was applied to the upper Tikovil River basin (55·6 km$^2$). It was tuned with the limited evidence of groundwater conditions during the monsoon season of 2005 and validated against observed landslide activity in the hydrological year 2001–2002. Given the data poor conditions in the region some modifications to the original model were in order, including the estimation of parameters on the basis of generalized information from secondary sources, pedo-transfer functions, empirical equations and satellite remote sensing data. Despite the poor input, the model captured the general temporal and spatial pattern of instability in the area. Sensitivity analysis proved root cohesion, soil depth and angle of internal friction as the most dominant parameters influencing slope stability. The results indicate the importance of root cohesion in maintaining stability and the critical role of the management of rubber plantations in this. Interception and evapotranspiration showed little influence on the development of failure conditions. The study also highlights the importance of high resolution digital terrain models for the accurate mechanistic prediction of shallow landslide initiation. Copyright © 2009 John Wiley & Sons, Ltd.

KEYWORDS: shallow landslides; debris flow; dynamic modelling; vegetation effects; root cohesion; data deficiency; STARWARS; PROBSTAB; Western Ghats

## Introduction

Landslides are an increasing concern in India due to the ongoing expansion of the population into hilly terrain. This migration is accompanied by the degradation of forested areas or their complete conversion to commercial and subsistence agriculture. Such changes in land-use/land-cover results in the loss of root reinforcement and the mitigating influence of the canopy through interception and evapotranspiration on the generation of critical pore water pressure conditions (Styczen and Morgan, 1995). Thus deforestation may lead to an increase in the spatial and temporal frequency of landslides (Glade, 2003; Ziemer, 1981), putting the population at an elevated risk. An area that experiences such an increase in landslide frequency is Kerala, the second most densely populated (819 people/km$^2$) state of India (Census of India, 2001). The Western Ghats, the most prominent orographic feature of peninsular India, occupies 47% of this state and the annual rainfall is as high as 5000 mm, concentrated during two monsoon seasons. This favours slope failures often resulting in debris flows.

Over the period of 1975 to 1995, it is estimated that landslides killed about 100 people and rendered about 600 families homeless along the Western Ghats (Thakur, 1996) whilst floods and landslides together have caused an estimated damage of 12 billion Euros in Kerala in 2007 alone (Murali Kumar, 2007). Inventories suggest that landslide frequency in Kerala has risen sharply since the onset of deforestation by migrant farmers in the 1940s (Gopinath, 1985). It is to be expected that landslide frequency will continue to rise given the rapid land-use changes in the highlands of Kerala (George and Chattopadhyay, 2001). Thampi *et al.* (1998) postulated that land-use practices related to rubber (*Hevea brasiliensis*) plantations may have aggravated the situation and tuber crops such as cassava (*Manihot esculenta*) are detrimental to slope stability as they lack root cohesion. Therefore, effect of vegetation on landslide activity under present-day conditions and for future scenarios of land-use/land-cover change should be included in landslide hazard assessments.

The effect of vegetation on slope stability may broadly be classified as either hydrological or mechanical in nature. Several studies have evaluated the effects of vegetation on slope stability, both in terms of the net precipitation inducing critical pore water pressure conditions (Gorsevski *et al.*, 2006; Wilkinson *et al.*, 2002) and in terms of mechanical effects, particularly root reinforcement (Bathurst *et al.*, 2007; Nilaweera and Nutalaya, 1999; Roering *et al.*, 2003).

Mechanical effects of vegetation comprise reinforcement of soil by roots, surcharge, wind-loading and surface protection.

Root-induced cohesion is identified as the most dominant of the beneficial mechanical effects (Greenway, 1987). Tree roots reinforce the soil shear strength by anchoring the soil layers and by forming a binding network within the layer (Schmidt *et al.*, 2001; Waldron, 1977; Ziemer, 1981).

The most significant beneficial hydrological effect of vegetation on slope stability is evapotranspiration (Greenway, 1987). This process prevents the build up of pore water pressure especially when water is contributed through distributed rainfall events and over days (Styczen and Morgan, 1995). Interception losses have a beneficial influence. However, increased infiltration in densely vegetated areas may reduce stability through rapid soil saturation (Greenway, 1987).

Assessment of slope hydrology using physically based models in the data poor setting of Indian catchments have been attempted by several authors (Immerzeel *et al.*, 2008; James *et al.*, 1981; Refsgaard *et al.*, 1992; Singh *et al.*, 2006) with varying success. However, there is a lack of quantitative assessments of vegetation effects on slope stability.

According to Varnes and IAEG Commission on Landslides and other Mass-Movements (1984) landslide hazard can be defined as the probability of occurrence of a potentially damaging landslide event within a given area in a given period of time. This probability is related to environmental factors like slope and hydraulic conductivity and dynamic factors like precipitation and runoff. In regions lacking historical data distributed physically based dynamic modelling is the most suitable method to derive the spatio-temporal probabilities of landslides (van Westen *et al.*, 2005). Unlike the statistical (e.g. Guzzetti *et al.*, 2005; Santacana *et al.*, 2003) and heuristic models (e.g. Barredo *et al.*, 2000; Castellanos Abella and van Westen, 2007), they are capable of quantitatively assessing the mechanistic influence of changes in environmental conditions on slope stability, for example those of vegetation (van Beek and van Asch, 2004). Several physically based models are available for simulating shallow landslide initiation, e.g. Stability Index Mapping (SINMAP; Pack *et al.*, 1998), SHALSTAB (Dietrich and Montgomery, 1998), SHETRAN (Ewen *et al.*, 2000), Transient Rainfall Infiltration and Grid based Regional Slope Stability (TRIGRS; Baum *et al.*, 2002), Storage and Redistribution of Water in Agricultural and Re-vegetated Slopes coupled with Probability of Stability (STARWARS+PROBSTAB; van Beek, 2002) and GEOtop-FS (Simoni *et al.*, 2008). Only few contain a dynamic hydrology component and still fewer allow the user to change the parameterization.

Here we demonstrate the scope and limitations of using data intensive physically based models in data poor environments to conduct reliable shallow landslide hazard assessment. Our attempt was to evaluate the sensitivity of slope stability to hydrological effects of vegetation and root reinforcement jointly with other intrinsic and extrinsic factors in the upper Tikovil River basin (Kerala, India) using a dynamic hydrological model coupled with a slope stability model.

## Study Area

The study area comprises the upper Tikovil River Basin, Kerala, India (Figure 1). It covers 55·6 km$^2$ in the centre of the southern segment of Western Ghats (Spate *et al.*, 1967).

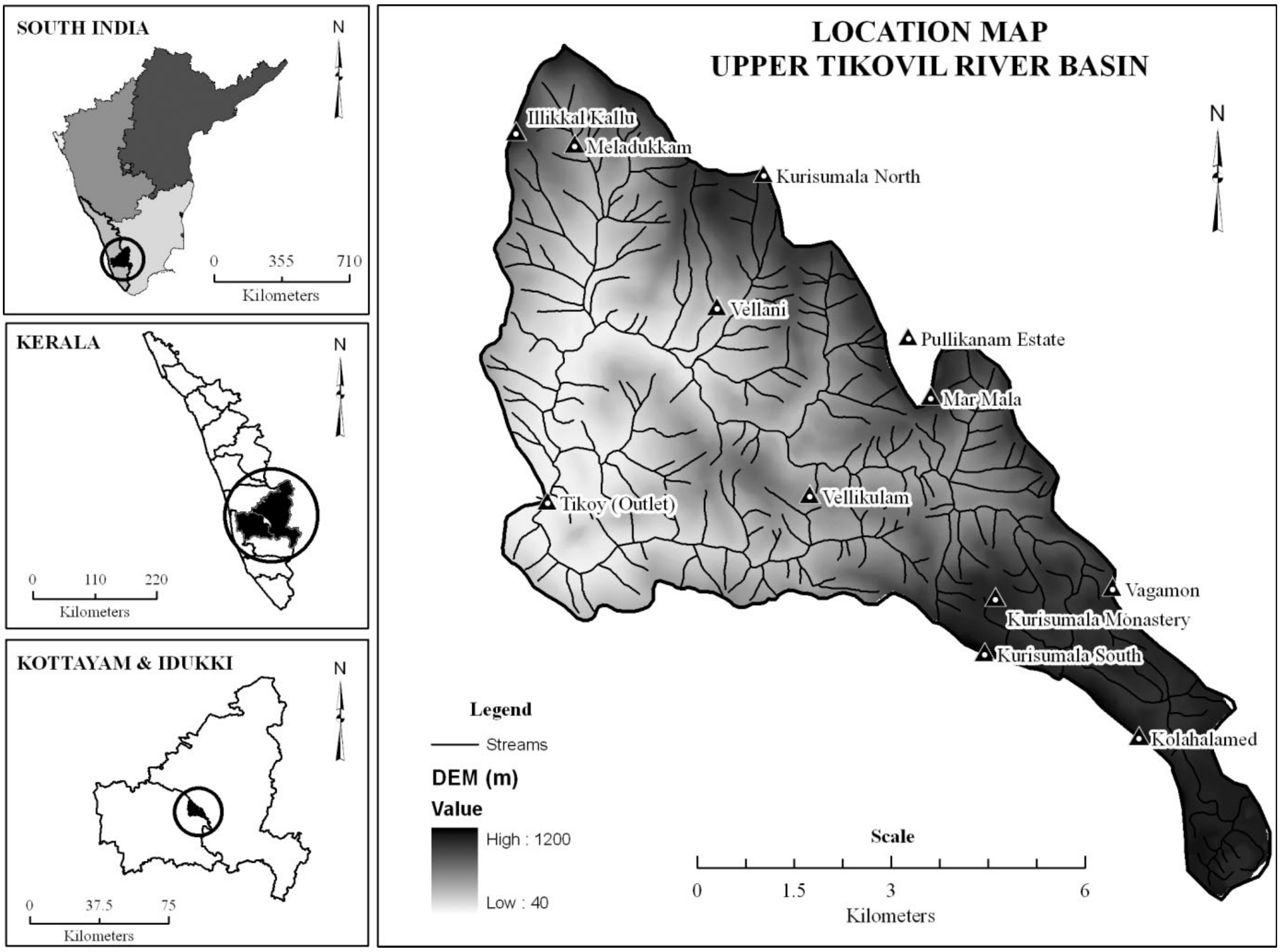


**Figure 1.** Relative location of the Tikovil River Basin which is administratively part of Kottayam and Idukki districts of Kerala state, south India, overlaid by the drainage network and some of the landmarks.

The Peerimed plateau, a peneplanation surface (Soman, 2002), forms an escarpment all along the eastern and northeastern part of the area. Chandrakaran *et al.* (1995) indicated that the area has thin sandy soils with low cohesion resting over hard crystalline Precambrian Charnockites.

Temperature of the area fluctuates between 16 °C to 36·5 °C annually. Based on rainfall measurements in the study area from 1965 to 1996, Thampi *et al.* (1998) concluded that the area follows the overall temporal distribution of rainfall in the state, with two monsoons following the pre-monsoon period. The average annual rainfall over the period 1960–2005 is 5426 mm, which is seasonally distributed as follows:

- South-west (SW) monsoon (June to September) – 4360 mm
- North-east (NE) monsoon (October to December) – 554 mm
- Pre-monsoon (January to June) – 511 mm

Widespread deforestation in the region started in the late 1880s (Victor, 1962). From the late 1970s almost the entire region was planted with rubber, except plateau tops and mountain ridges owing to unfavourable climatic conditions and insufficient soil depth. In-sloping terraces bounded with stone-packed earthen walls are constructed across the slope direction (at least every 2 m contour interval) for planting rubber (Figure 2(left)). A land-use/land-cover map prepared by Thampi *et al.* (1998) shows that 55% (31·13 $km^2$) of the area was occupied by rubber plantations in 1998. Apart from rubber other main land-cover types are wild grasslands (8·23 $km^2$, 14%), degraded forest (4·55 $km^2$, 8%), grazing pastures (4·04 $km^2$, 7%), tea plantations (3·29 $km^2$, 5%), mixed crops (1·5 $km^2$, 2%) and rock outcrops (3·08 $km^2$, 5%).

Rubber has a crop life of ~20 years, after which it has to be renewed. As plantations pass their optimal crop life, they are felled, exposing the soil. Thus, although the map of the region represents the land-use conditions adequately, the actual land-cover conditions are unknown as a plot may be bare for several years every two decades when the replanted rubber trees are growing (Sankar, 2007).

Almost every year the area experiences numerous debris flows during the monsoon seasons. The oldest known landslide event in the study area occurred on 4 October 1882 near Meladukkam (Figure 1) (Souvenir Committee, 1982). Based on a landslide inventory map by Thampi *et al.* (1998), out of the 34 landslides mapped, 28 occurred in rubber plantations, two occurred in the grasslands and four in degraded forests. A total of 16 additional landslides were mapped during the SW monsoon season of 2005, out of which 11 occurred on 8 July 2001 and five occurred in 2000 for which reliable records of the date of occurrence was not available. All the located flows in the region have their origin at altitudes >300 m above sea level (a.s.l.), and on slopes >20° (Kuriakose *et al.*, 2008a). Harikrishnan *et al.* (1995) revealed that the locations of slope failure (Figure 2(right)) have the typical characteristics of hollows, with colluvial material accumulated in depressions mostly adjoining steep rocky exposures. The plain of failure is often the contact between the soil and the bedrock.

The hollows if undisturbed support evergreen creepers, thorny shrubs and bamboo. They are the source areas of first-order ephemeral streams and rills which convey surplus surface runoff during extreme rainfall events. In order to gain more cultivable land and trap the much valuable top soil, farmers create terraces in the upper slopes often ignoring these hollows and rills. As soil accumulates in the hollows farmers clear the natural vegetative cover, terrace and plant tuber crops. Unlike those for planting rubber, these terraces in the upper slopes are constructed with loosely stacked rock fragments.

Several landslides are known to have initiated in these hollows mostly after clearing the natural vegetation. Though the locations of landslides are known, the date and time of occurrence of most of these events are unknown. Debris flows that occur as a consequence of these landslides are confined to the existing drainage lines and widen the streambeds that they follow, causing significant crop destruction along the path.

## The Model

The models used for the study were developed by van Beek (2002). They comprise a distributed dynamic hydrological model (STARWARS) that is coupled to a stability model (PROBSTAB) (Figure 3). The dynamic spatial outputs of the hydrological model are the inputs for the slope stability model. An added

**Figure 2.** Terraces with young rubber saplings and pineapple (left); a typical hollow in the region that adjoins a rocky exposure (right).



DOI: 10.1002/esp

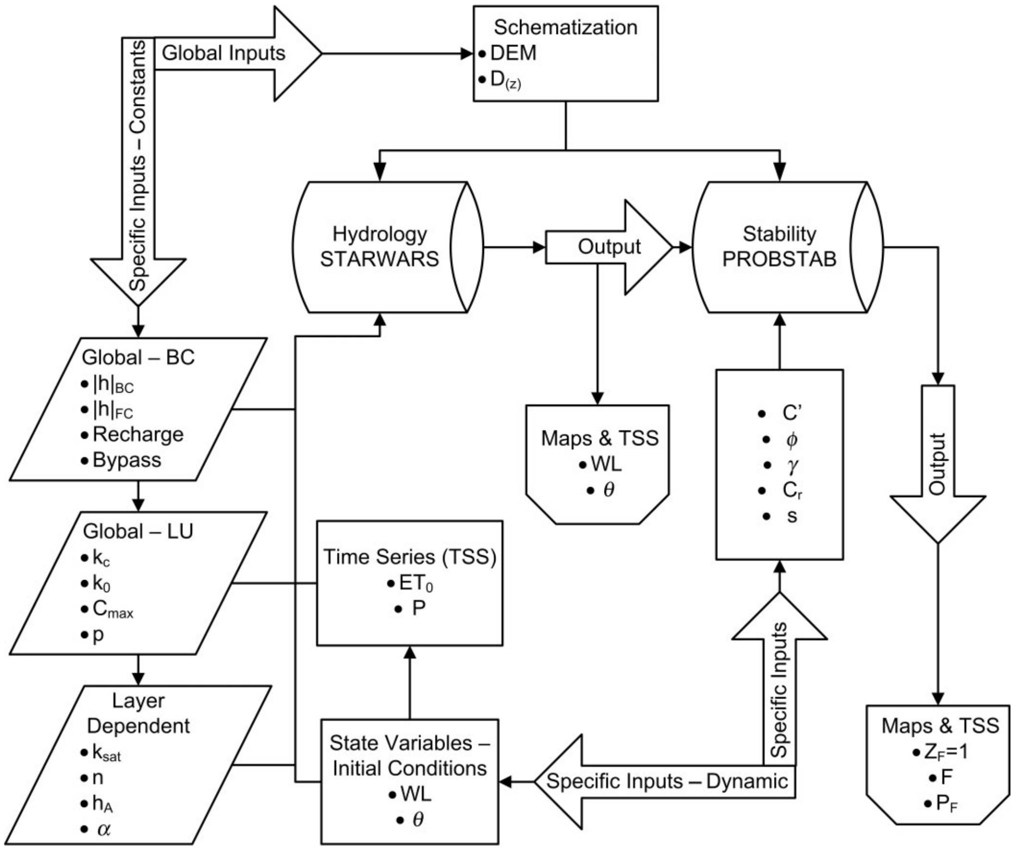


**Figure 3.** General framework of the STARWARS and PROBSTAB models (cf. Table I for explanation).

advantage of the models is that its open architecture allows modification of the model script and thereby enables different parameterizations appropriate for the study area. This is crucial in data poor regions such as the study area where several parameters may have to be derived from secondary sources. Both the models are embedded in PCRaster®, a geographic information system (GIS) with an advanced Environmental Modelling Language (http://www.pcraster.nl). A detailed description of the model theory and its schema can be found in van Beek (2002) and Malet *et al.* (2005). A brief outline is provided below.

STARWARS was originally designed to evaluate the effects of vegetation on hillslope hydrology in southeast Spain. Soil hydrological properties (Table I) can be assigned to specific land-use types and the model originally included the processes of interception and evapotranspiration. The amount of actual evapotranspiration is scaled to the available storage and Food and Agricultural Organization (FAO) crop factors (Doorenbos and Pruitt, 1977). It contains a detailed description of the unsaturated zone that is present in the soil mantle over a semi-impervious lithic contact, which in this case is the Charnockites. The soil profile is subdivided into three layers that can be interpreted as the A, B and C horizons. Percolation of soil moisture is driven by gravity and depends on the unsaturated hydraulic conductivity which is prescribed by the soil water retention curve of Farrel and Larson (1972) and the unsaturated hydraulic conductivity relationship of Millington and Quirk (1959). At the lower end of the soil mantle, the percolation into the underlying bedrock is impeded and a perched water table may form. The resulting perched water table will drain laterally according to the gradient of the phreatic surface. All unsaturated fluxes are considered to be vertical only.

PROBSTAB is based on the infinite slope model and as such is valid for translational slides (Skempton and DeLory, 1957). This is consistent with the type of failures in the study area. PROBSTAB calculates Factor of Safety (FOS) at the contact between the soil and the bedrock based on the daily variation of water level and volumetric moisture content, which are the output of STARWARS. In addition, PROBSTAB uses the matric suction to calculate the unsaturated shear strength when a perched water table is absent using Fredlund's (1987) equation and it includes the mechanical effects of root reinforcement and surcharge on slope stability. Hence the calculated stability varies on a day-to-day basis with the hydrological input. Probability of failure was obtained using the first-order second moment (FOSM) approach (Ang and Tang, 1984) which takes into account the uncertainty in the estimation of the mechanical effects of vegetation, shear strength parameters, soil depth and slope angle. FOSM method necessitates the assumption of a normal curve. The curve is implemented in the model with the first standard deviation on the positive and negative side for a given parameter. This draws from the assumption that by using the first standard deviation on either sides of the curve, 66'6% of the total possible variation of the parameter is captured. This is also a direct indicator of the sensitivity of the model to the parameter and thus can also partially address the issue of uncertainty in parameter estimation. Slope hydrology was not treated as an independent parameter for calculating the probability of failure.

Owing to the data poor situation some modifications to the models and their dependency were made. For example, potential evapotranspiration (PET) was calculated outside the model environment using Hargreave's equation (Hargreaves and Samani, 1982) which is less data demanding than the Penman's equation (Penman, 1948) originally used in the model by van Beek (2002). Interception was computed by means of 'Aston's (1979)' equation (see Equation 1), and throughfall and evapotranspiration of the canopy storage was addressed outside the model environment. Table I provides the list of parameters



DOI: 10.1002/esp

**Table I.** Overview of parameters required for the STARWARS and PROBSTAB models

| Parameter | Type | Values/classes | Obtained from |
|---|---|---|---|
| DTM (Digital Terrain Model, a.s.l) | Spatial | 628·5 m [400] | Survey of India Topographic Sheet |
| $D$(z) (Soil thickness from bedrock including saprolite) | Spatial | 2 m [1·6] | Field surveyed, interpolated, topographic adjusted and spatially aggregated with a range of 0·25 m by Thampi *et al.* (1998), field verified for the present research (see Figure 4a) |
| LU (Land use/land cover) | Spatial | 7 classes | Aerial photo interpretation and satellite imagery interpretation by Thampi *et al.* (1998); field verified for the present research |
| $\|h\|BC$ (Matric suction under the lithological contact which is the lower boundary condition) | Constant | 3 m | Literature value (Kutılek and Nielsen, 1994) |
| $\|h\|FC$ (Matric suction at field capacity) | Constant | 1 m | Literature value (Kutılek and Nielsen, 1994) |
| $k_c$ (Crop factor) | Spatial | 0–1[a] | Food and Agricultural Organization (Doorenbos and Pruitt, 1977), constant for a land use |
| $k_0$ (Infiltration capacity) | Spatial | 0·4 m/day | Derived as proportional to saturate hydraulic conductivity of the top soil layer and varies with soil type |
| $C_{max}$ (Canopy storage) | Spatial | 0·02 m | Derived based on Von Hoyningen-Huene (1981) using LAI computed from MODIS NDVI 16 day composites; this was an input to the Aston's equation used for computing interception |
| $P_r$ (Throughfall ratio) | Constant | 0·5[a] | Derived in relation to LAI as suggested by van Beek (2002) |
| $k_{sat}$ (Saturated hydraulic conductivity) | Spatial | 0·2 m/day | Derived using Rosetta (Schaap, 1999) based on textural properties and bulk density estimated by Thampi *et al.* (1998), varies with soil type and depth |
| $k_{sat}BC$ (Saturated hydraulic conductivity boundary condition which is the lower boundary condition) | Spatial | 0·008 m/day | Derived using Rosetta (Schaap, 1999) based on textural properties and bulk density estimated by Thampi *et al.* (1998), set as the $k_{sat}$ of the soil layer in contact with the bedrock |
| $n$ (Porosity) | Spatial | 0·4 $m^3/m^3$ | Derived in relation to bulk density; bulk density from Thampi *et al.* (1998), varies with soil type and depth |
| $h_A$ (Air entry value) and $h_ABC$ (Air entry value at the lithological contact which is the boundary condition) | Constant | 0·06 m | Derived for Farrel and Larson based on van Genuchten parameters as obtained from Rosetta (Schaap, 1999), constant across the soil depth |
| $\alpha$ (Slope of the soil water retention curve) | Spatial | 10·2 m | Derived for Farrel and Larson based on van Genuchten parameters as obtained from Rosetta (Schaap, 1999), varies with soil type |
| $\tau$ (Tortuosity parameter for Millington and Quirk) | Constant | ¾[a] | Literature value (Kutılek and Nielsen, 1994) |
| $ET_o$ (Potential evapotranspiration) | Aspatial, daily variation | 0·003 m/day | Derived outside the model using Hargreaves equation with data obtained from Kurisumala Monastery (KM; 0·5 km from the study area), Rubber Research Institute of India (RRII; 30 kms from the study area) and Indian Meteorological Department (IMD; 30 kms from the study area) |
| $P$ (Precipitation) | Aspatial, daily data | ~5 m (Annual) | Obtained from KM (daily data from 1999–December 2001), RRII (daily data from 2002 to 2005) and Pullikanam Tea Estate (PTE, Seasonal totals from 1990 to 1998) |
| $WL_i$ (Initial water level from bedrock) | Spatial | ~2 m/h/$m^2$ | $WL_i$: from long term model runs based on average $P$ and ET conditions |
| $\theta_i$ (Initial volumetric soil moisture content) | Spatial | ~0·45 $m^3 m^{-3}$/h | $\theta_i$: from long term model runs based on average $P$ and ET conditions |
| $C'$ (Soil cohesion) | Spatial | 0·0012 MPa [0·0006] | Triaxial test results from Thampi *et al.* (1998), varies with soil type |
| $\phi$ (Angle of internal friction) | Spatial | 33·8° [6·2] | Triaxial test results from Thampi *et al.* (1998), varies with soil type |
| $\gamma$ (Bulk unit weight) | Spatial | 15·3 kN/$m^3$ [1·4] | Test results from Thampi *et al.* (1998), varies with soil type |
| $s$ (Bulk unit weight of vegetation) | Constant | 0·3 kN/$m^3$ [0·3] | Field interview, collected only for rubber |
| $C_r$ (Root cohesion) | Spatial | 0·007 MPa [0·01] | Calculated using measured tensile strength of rubber roots and related to other land-use types based on soil depth and root density |

[a] Dimensionless.

*Note*: Standard deviation values of those parameters used in the sensitivity analysis (first-order second moment, FOSM) are given in square brackets. For a detailed description of the equations used in the model refer to Kuriakose (2006), Malet et al. (2005) and van Beek (2002).



DOI: 10.1002/esp

necessary for STARWARS and PROBSTAB and the methods utilized to obtain them for the present research. All spatial data had a resolution of 20 m by 20 m.

Calibration and validation are two crucial necessities in using models for simulating earth surface processes (Karssenberg, 2002). Availability of calibration and validation data determined the model simulation period and time steps used in this study. Calibration of slope hydrology required simulations from 1990 to 2006. Validation was done by comparing slope stability simulation for the year 2001 with the actual record of landslides. A six hour time step was used to simulate slope hydrology, though the results were aggregated to daily time steps for use in the slope stability simulation.

## Model Parameterization

Data were lacking for most of the parameters at the start of the research. Therefore it was decided to evaluate the scope of parameterizing the models using maps, satellite data, pedotransfer functions and literature derived values to arrive at estimates of the necessary parameters in the field scale. Lack of historical data forced us to assume all parameters except the climatic variables as constant throughout the model simulation period. This resulted in ignoring the crop cycle of the rubber plantations that may have occurred during the model simulation period.

The data available were daily rainfall, crop factors, potential evapotranspiration, MODIS NDVI 16 day composites, soil types, soil properties, contour map from topographic sheet, soil depth, root cohesion, soil depth, root cohesion, land-use/land-cover and a rudimentary landslide inventory containing only the date and the location of events (cf. Table I for sources).

### Climatic parameters

As landslide initiation in the region is driven by a sharp rise in the pore water pressure following net precipitation input (Basak and Narasimha Prasad, 1989), evapotranspiration and rainfall data with fine temporal resolution (minutes to hours) was required. However, only coarse temporal resolution (days to seasonal totals) climatic data was available from three different sources [Rubber Research Institute of India (RRII), Kurisumala Monastery (KM) and Pullikanam Tea Estate (PTE); Table I]. These data sets were not continuous for the entire modelling period (1990–2005).

For the period 1990–1998 we relied on synthetic rainfall which was generated by redistributing available seasonal totals proportionally to the daily rainfall totals of 1999 to 2002, with normal and leap years being treated separately. The partial record of daily rainfall of 2002 was completed with the daily rainfall from 1 January to 31 May 2002 available from RRII (cf. Table I). Daily rainfall data was available for the first 10 months of the calendar year 2005 constituting the calibration period. Daily averages of the available records were used to fill the gap from November 2005 to May 2006. Thus, a complete record of daily rainfall from 1990 to 2005 was constructed. These records were organized per hydrological year, commencing with the season of soil moisture recharge, and concluding with the completion of the season of maximum evapotranspiration (Glickman, 2000). The hydrological year in Kerala starts on average on 1 June, with a standard deviation of 8 to 9 days, and runs to 31 May of the subsequent calendar year (Fasullo and Webster, 2002).

Solar radiation and temperature values were available from RRII for a period from 2002 to 2005. Daily Reference PET (RPET) values were computed from these data and used for the entire modelling period (1990–2006) assuming that evapotranspiration on a wet day is negligible given the monsoonal climate and cloudiness of the region. Potential evapotranspiration is at its maximum from December until April while May receives the pre-monsoon showers and thus lacks any significant transpirational loss. The average annual PET of the region is 1600 mm.

### Hydrological effects of vegetation

The land-use/land-cover map (Thampi *et al.*, 1998) was one of the fundamental inputs for the modelling, specifying interception and evapotranspiration losses as well as the distribution of root cohesion and permeability amongst others. In order to assess the applicability of the available land-use/land-cover map to the calibration year, 25 random locations covering the entire study area were selected. Out of the 25 points, 21 had the same land-use/land-cover as that of the mapped land-use/land-cover, while four disagreed, due to crop rotation in rubber plantations and conversion to built-up area. Interception was computed with Aston's equation (Equation 1) using satellite data (MODIS NDVI 16 day composites) for 2000 and 2001, daily precipitation for the respective years and the crop factors of the land-use/land-cover.

$$S = f_c S_{\max}\left(1 - \exp^{-k\frac{P_{cum}}{S_{\max}}}\right) \tag{1}$$

where, $S$ is the interception (in mm), $f_c$ is the fractional vegetation cover (dimensionless), $S_{max}$ the maximum canopy storage (in mm), $-k$ the correction factor for vegetation density, and $P_{cum}$ the cumulative rainfall (in mm).

The MODIS NDVI was used to compute Fractional Vegetation Cover from which Leaf Area Index was derived using the method proposed by Walthall *et al.* (2004). The extinction factor, $k$, of Aston's equation was computed as 0·046LAI. Maximum canopy storage was computed from LAI using the equation proposed by Von Hoyningen-Huene (1981) (Equation 2).

$$S_{\max} = 0{\cdot}935 + 0{\cdot}498LAI - 0{\cdot}00575LAI^2 \tag{2}$$

Given the monthly values of fractional vegetation cover, canopy storage and extinction factor, daily interception was computed from daily cumulative rainfall data using a model created in PCRaster. By using this method interception could be quantified for each day in the original grid resolution of 250 m × 250 m, which was re-sampled (nearest neighbour method) to the model resolution of 20 m. The re-sampling was done for compatibility with other datasets and thus it did not improve (or degrade) the overall estimate of interception based on the original grid resolution of the MODIS NDVI data. The advantage of this parameterization was that it is continuous in time and space (van Westen *et al.*, 2008). Thus it enables to overcome the generalization of using individual parameters linked to land-use/land-cover maps with sharp class boundaries. It was observed that interception is highly sensitive to fractional vegetation cover of the area. A detailed description of the methods and the sensitivity analysis is available in (Kuriakose *et al.*, 2006).

All remaining (non-intercepted) rainfall was assumed to be reaching the surface while any canopy storage was made



DOI: 10.1002/esp

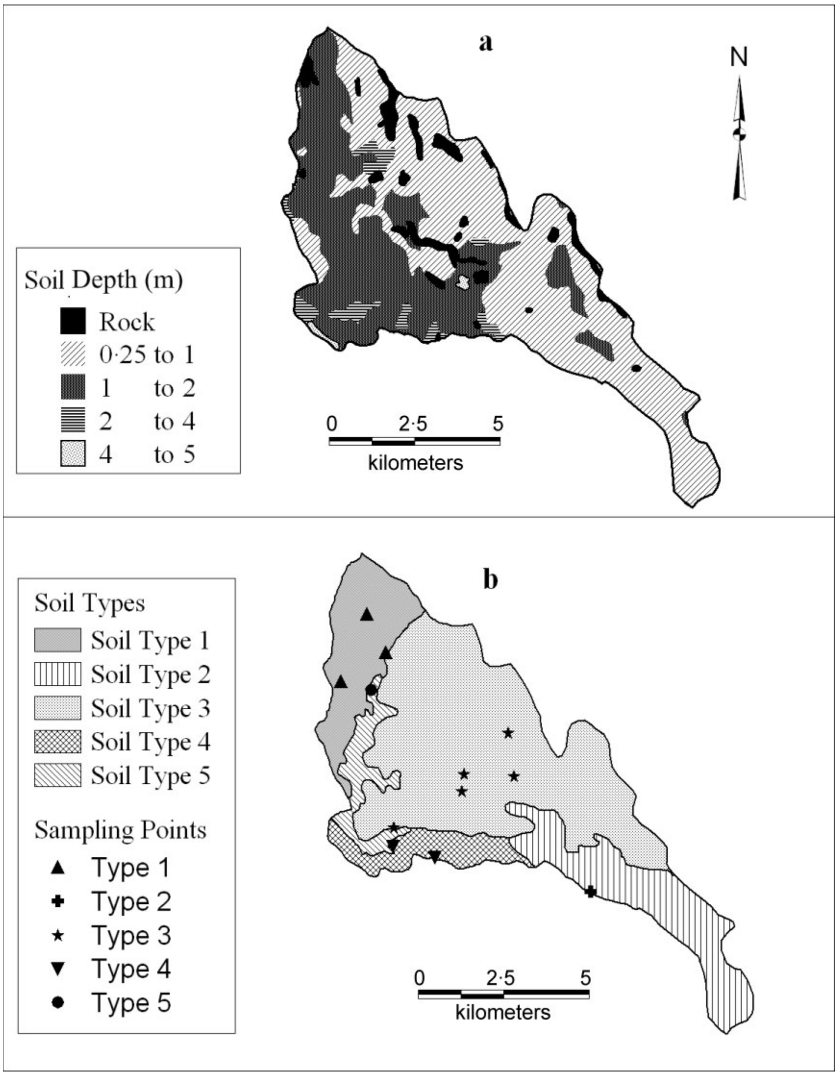


**Figure 4.** (a) Soil thickness based on Thampi *et al.* (1998); (b) soil types based on NBSS and LUP (1999) and soil sampling points of Chandrakaran *et al.* (1995).

available for evapotranspiration. RPET was adjusted to crop-specific PET using crop factors of the respective land-use types. All RPET exceeding the available canopy storage in a given day was assumed to be the fraction of PET that is to occur from the soil (FPET). Thus the outputs of this model were the daily effective rainfall and the FPET. These results were used as dynamic inputs for STARWARS. Within STARWARS, evapotranspiration occurs at the actual rates (which is FPET adjusted to crop factors) when the soil is close to saturation; else FPET was scaled down linearly depending on the soil moisture content in a given time step.

## Topographical and pedological data

A contour map with 20 m equidistance was used to generate a digital terrain model with a horizontal resolution of 20 m. A soil depth map was available from Thampi *et al.* (1998). This map was prepared from interpolated field measurements adjusted to topographic conditions and aggregated as discrete polygons with soil depth class intervals of 0·25 m (Figure 4a). For the modelling each polygon was assigned the upper limit of the respective class boundary. Its accuracy was assessed at the same 25 points used for the verification of the land-use map; the soil depth at 15 points differed from the prescribed values by less than 0·25 m, while 10 showed an error of 0·5 m or more.

The soil profile in a grid was schematized as three or two layers depending on the soil depth in that grid. A three layer schema constituted 30%, 50% and 20% to 5% of the soil depth to bedrock. A two layer schema was adopted, if the third layer derived in a pixel was <5% of the total soil depth. These schematizations were arbitrary as no depth wise information was available for any of the soil properties. Laboratory measurements of the geotechnical properties of soils in the area were available only for 12 points which were assigned to a soil type map (NBSS and LUP, 1999) with five soil units (Figure 4b). Given the scarcity of data, uniform values of cohesion, angle of internal friction (AIF) and bulk unit weight were assigned to each unit.

No information on soil hydrological properties were available. Saturated hydraulic conductivity ($k_{sat}$) of individual soil units were derived by means of the pedo-transfer functions in the ROSETTA (Schaap, 1999) package using textural properties and bulk density. ROSETTA implements five hierarchical transfer functions (PTFs) for the estimation of water retention, and the saturated and unsaturated hydraulic conductivity (Schaap *et al.*, 2001). The models allows the estimation of van Genuchten water retention parameters (van Genuchten, 1980) and the saturated hydraulic conductivity using soil texture,



DOI: 10.1002/esp

**Table II.** Soil textural, hydrological and mechanical properties

| Parameters | Soil units | | | | |
|---|---|---|---|---|---|
| | 1 | 2 | 3 | 4 | 5 |
| Sand % | 40 | 50 | 40 | 40 | 50 |
| Silt % | 20 | 15 | 20 | 25 | 20 |
| Clay % | 40 | 35 | 40 | 35 | 40 |
| Bulk unit weight (kN/m$^3$) | 13·0 | 16·3 | 15·9 | 16·4 | 14·7 |
| Porosity ($n$) (m$^3$/m$^3$) | 0·5 | 0·4 | 0·4 | 0·4 | 0·4 |
| Air entry value ($h_A$) (m) | | | 0·06 | | |
| SWRC slope ($\alpha$) | 9·1 | 11·0 | 10·7 | 10·4 | 9·7 |
| Cohesion (MPa) | 0·0016 | 0·036 | 0·0013 | 0·0013 | 0·0023 |
| Angle of internal friction (deg) | 25·0 | 33·7 | 39·9 | 39·2 | 31·0 |
| $k_{sat}$ Layer 1 (m/day) | 0·7 | 0·3 | 0·4 | 0·3 | 0·5 |
| $k_{sat}$ Layer 2 (m/day) | 0·2 | 0·09 | 0·1 | 0·08 | 0·2 |
| $k_{sat}$ Layer 3 (m/day) | 0·013 | 0·006 | 0·009 | 0·005 | 0·010 |

bulk density and/or one of two water retention points. Parameters of the van Genuchten soil water retention parameters were obtained with ROSETTA and used to fit the Farrel and Larson (1972) soil water retention curve parameters, they being, slope of the soil water retention curve ($\alpha$) and air entry value ($h_A$). Porosity ($n$) was derived as the complement of volume taken up by solids using dry bulk density and mean particle density (2·7 gm/cm$^3$). Table II shows soil textural, hydrological and mechanical properties as applied to each soil unit.

Soil hydrological properties (Tables I and II) were linked to the five soil types and seven land-use/land-cover classes, yielding a cross-table of 35 combinations. For each of the combined classes, the parameters, $k_{sat}$, $n$, $h_A$ and $\alpha$ were specified for the (two or) three soil layers (Table II), although a vertical stratification was assumed only for the estimated $k_{sat}$, the others remaining constant with depth. The calculated value of $k_{sat}$ was assigned to the third layer and increased exponentially so that the uppermost layer had a 50% higher $k_{sat}$. This was done based on the assumption that the saturated hydraulic conductivity increased towards the surface as a result of biological activity. Although this increase was plausible and evident in the field, we reiterate that this parameterization was based solely on expert judgement.

## Mechanical effects of vegetation

Root reinforcement was calculated using the conceptual relationship suggested by Schmidt *et al.* (2001) based on the evidence of landslide activity in Oregon following earlier works by Waldron (1977) and Wu *et al.* (1979) (Equation 3).

$$C_r = a\sum_{i=1}^{n} T_{ri}\left(\frac{A_{ri}}{A_s}\right) \tag{3}$$

where, $C_r$ is the root-induced cohesion for a given species, $T_{ri}$ is the tensile strength of an individual root for a given type of vegetation, $A_{ri}/A_s$ is the proportion of root cross-sectional area to soil cross-sectional area, and $a$ the mobilized tensile resistance in root fibres (Equation 4), which is:

$$a = \cos\chi \tan\phi + \sin\chi \tag{4}$$

in which $\phi$ is the AIF of the soil and $\chi$ is the angle of shear of the roots.

The value of $a$ as established by Wu *et al.* (1979) is 1·2 for $25° < \phi < 45°$ and $40° < \chi < 70°$. As the $\phi$ values of the study area were comparable (Table II) with that for which Wu *et al.* (1979) estimated the value of $a$, this value was assumed to be applicable for computing the $C_r$ in the study area. The $T_{ri}$ of roots from a 23 year old rubber tree was measured using a universal testing machine generally used for testing the tensile strength of fibres. Only 15 root samples with a diameter ($x$) of >8 mm were tested, given the limitation of root breaking due to clamping. All root samples were ~15 cm long. Both ends of each sample were covered with thin cotton cloth to ensure necessary grip during the test. Figure 5 shows this regression relationship, which has the form,

$$T_{ri} = 8{\cdot}5148e^{-0{\cdot}0143x} \tag{5}$$

Average root count in a rubber plantation was worked out based on root counting in 1 m$^2$ pits extending to the bedrock and literature derived values (Srinivasan *et al.*, 2004) for soil depths varying from 0·25 to 5 m in a class interval of 0·25 m. Root count for a given soil depth class is the average number of roots on all sides of the pit within that soil class. The root count at the bottom of the pit was also used to calculate the average root count of the deepest soil depth class in a pit. Thus the average root count distribution (Figure 6) represents the depth averaged lateral and basal root count with respect to soil depth. For the number of root counts in each soil depth, the corresponding root area was calculated assuming an average root diameter of 5 mm. This value approximates the average root diameter as Srinivasan *et al.* (2004) observed that ~80% of roots found in any depth in a rubber plantation is less than 2·5 mm in diameter. The values of $T_{ri}$ of a 5 mm root was calculated as 7·9 MPa from Equation 5. This value was an underestimate compared with the value (12·5 MPa) measured by Nilaweera and Nutalaya (1999) for rubber plants in Thailand.

From the calculated values of $A_{ri}/A_s$ and tensile strength, $C_r$ at various soil depths were derived. The arrived relationship between root count and soil depth in the rubber grown area was applied to other land-use types with a reduced arbitrary root count distribution, except for rocks where no root cohesion was applied. The value of $C_r$ is significant only if rubber roots can reinforce the soil by anchoring to the bedrock. Here, it is assumed that all rubber trees have roots that penetrate the bedrock and that these roots fail due to tension, prior to complete slope failure. However, field observations in the rubber plantations revealed that not all rubber trees had roots penetrating bedrock fissures whereas it can be expected that some penetrating roots might fail by pull-out rather than



DOI: 10.1002/esp

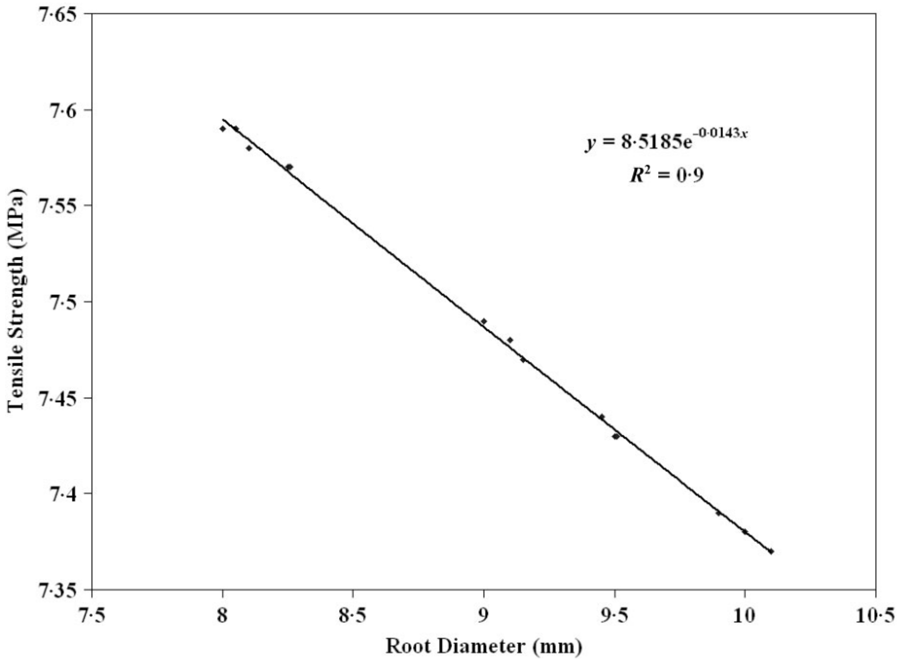


**Figure 5.** Relationship between root tensile strength and root diameter.

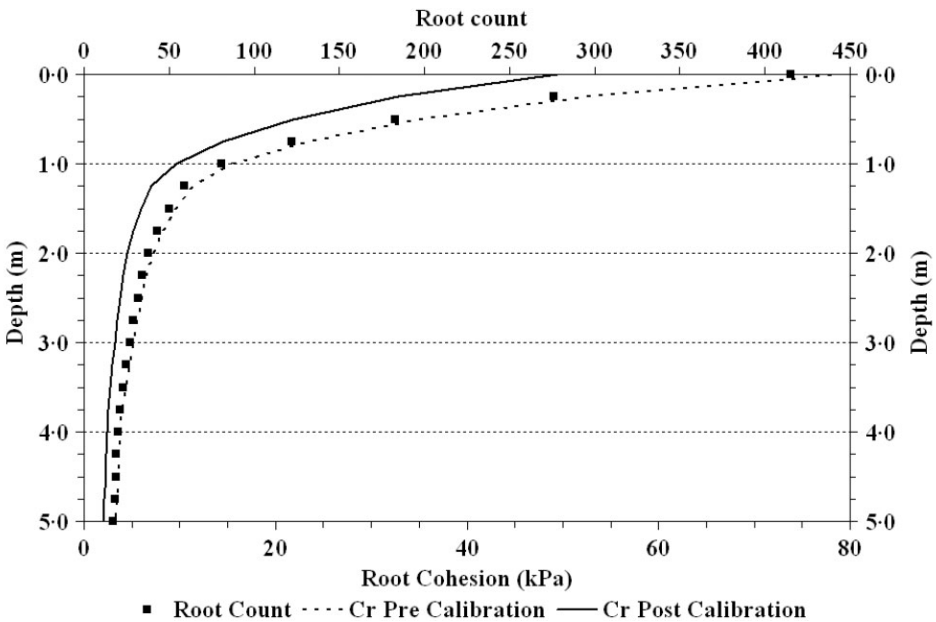


**Figure 6.** Depth averaged root count (lateral and basal) based on measured values and Srinivasan *et al.* (2004), and root cohesion before (pre) and after (post) calibration.

breakage at lower loads. Hence, the applied $C_r$ should be considered as an upper limit to the available strength.

The weight of an individual fully grown rubber tree was estimated to be about 550 kg based on information from planters. On average 20 trees are planted within a 400 $m^2$ area (the size of a pixel of 20 m by 20 m used in the research), resulting in a stress of 27·5 kg/$m^2$ or 0·0003 MPa. Root cohesion and surcharge variations with respect to the age of the tree were ignored.

## Calibration and Validation

Calibration of STARWARS was constrained to the SW monsoon season of the hydrological year 2005–2006 as groundwater observations were available only for this period. Initial conditions for this period was estimated by warming up the model for 10 average years (called the spin-up period) followed by the 15 actual hydrological years (1990–2005). Starting from the initial conditions of the spin-up period, the model was run in a six hour resolution, all outputs being subsequently processed as daily values. First, the hydrological model was calibrated against the water level during the SW monsoon period of 2005 measured in 11 open wells widely distributed in the study area. Soil depth was chosen as the parameter for calibration because of its highly variable and erratic nature. It was modified by increments of 0·01 m until the overall absolute error was at its minimum. The best fit was obtained with an increase of 0·08 m, baring the exposed rock surfaces, ($R^2$ = 0·7) between the observed and predicted water levels. Some amount of compensating error in this calibration value of soil depth may be a consequence of the use of daily resolution climatic data which cannot be quantified separately due to



DOI: 10.1002/esp

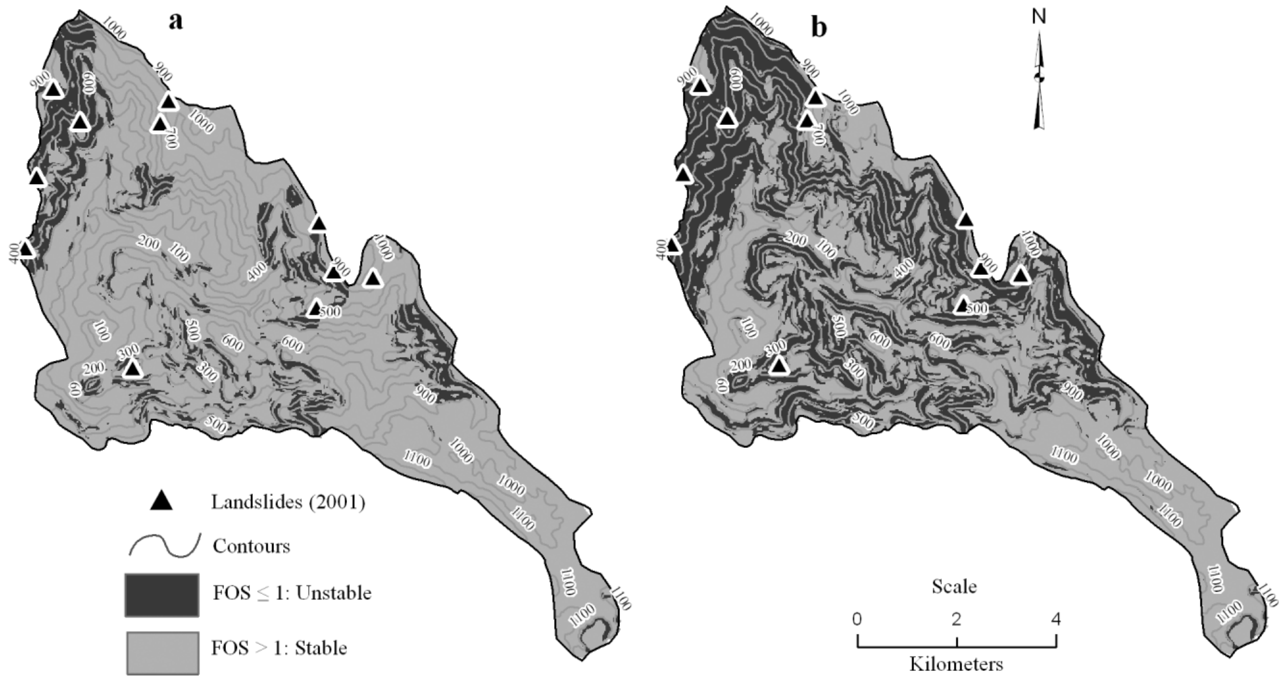


**Figure 7.** Actual locations of shallow landslides plotted over predicted slope instability (a) considering root cohesion and surcharge of vegetation and (b) without considering root cohesion and surcharge of vegetation.

the lack of fine resolution rainfall data. The root mean square error of the prediction was 0·29.

The stability model was calibrated at the known landslide locations assuming completely saturated conditions. The use of the original $C_r$ values resulted in unrealistically high stability, clearly pointing towards an overestimation of overall cohesion. This may be mainly due to the original over estimation of $T_{ri}$.

To obtain a better estimate of root cohesion, a back-analysis was employed, assuming that root cohesion suffices to maintain the safety factor at unity at the 50 known shallow landslide locations in the area. Any cohesion in addition to soil cohesion was considered to be provided by the roots. Optimization concerned the $T_{ri}$ of a 5 mm root. Prior to calibration, only six known initiation locations were predicted as failed whereas after calibration, with $T_{ri} = 6{\cdot}1$ MPa, 22 locations were predicted correctly. Figure 6 shows the relationship of $C_r$ with soil depth, before and after root cohesion calibration. The method provides only a practical approximation of root cohesion with the given data as it lumps all uncertainty into the tensile strength.

Subsequently, the calibrated STARWARS was applied to the hydrological years 1990–2001. Reliable landslide inventory containing information of the locations (cf. Figure 7) and day of events (11 landslides on 8 July) was available only for the hydrological year 2001–2002, thus limiting the temporal validation of slope stability simulations. As the target was to assess model capability in simulating slope instability with an accuracy of days, a daily time step was chosen. Spatial validity of the model results of 2001 to 2002 was assessed using the ratio of area predicted as failed to area that actually failed. An evaluation of the effect of vegetation on slope stability was attempted by applying the model to the data set of the hydrological year 2001–2002, with and without considering $C_r$ and surcharge as parameters.

## Model Performance for 2001

The region received a total rainfall of 3179 mm during the SW monsoon season of 2001. Of this, 238 mm was on 8 July. This was preceded by 1494 mm rainfall from the start of the season on 1 June. The first 10 days of September 2001 was rainless. These intermittent rainless periods in the monsoon known as monsoon breaks are significant in reducing soil moisture (Kusuma *et al.*, 1991). Figure 8 shows the response of water level to rainfall as predicted by the model for one of the known landslide initiation locations. The prediction is an over estimation of the critical slope hydrology conditions as it is only on the day of failure that the peak water level was expected.

From the results it can be inferred that pore water pressure in the region responds quickly to wet and dry periods and the soil is saturated very rapidly. The spontaneous response of pore water pressure to rainfall events can be attributed to the fairly permeable soils in the region (Table II). This result corroborates earlier findings from the region (Basak and Narasimha Prasad, 1989; Langsholt, 1992).

In the present research temporal validity of the model was assessed with the failures that occurred on 8 July 2001. Eight of the 11 failure locations were predicted by the model as failed (FOS ≤ 1) on the day and these locations were also predicted to be having a $P(\mathrm{FOS} \le 1) \ge 60\%$ (Table III).

## Results and Discussion

Figure 7 shows predicted instability overlaid by the 11 known landslides for the year 2001–2002 with (Figure 7a) and without (Figure 7b) considering the mechanical effects of vegetation. The model predicted 14% (8 $km^2$) of the area as unstable during the monsoon seasons against the actual <1% (0·0044 $km^2$) area. Out of this 8 $km^2$, 1·17 $km^2$ remained unstable throughout the year while the rest of the region experienced instability as a consequence of the development of critical slope hydrological conditions. Without mechanical effects incorporated 42% (23·3 $km^2$) of the study area was predicted as unstable.

The simulated area of instability was an overestimation (cf. Figure 7a) which is evident from the difference between the predicted area of failure and actual area of failure. However, the fact that eight out of 11 known landslide locations were



DOI: 10.1002/esp

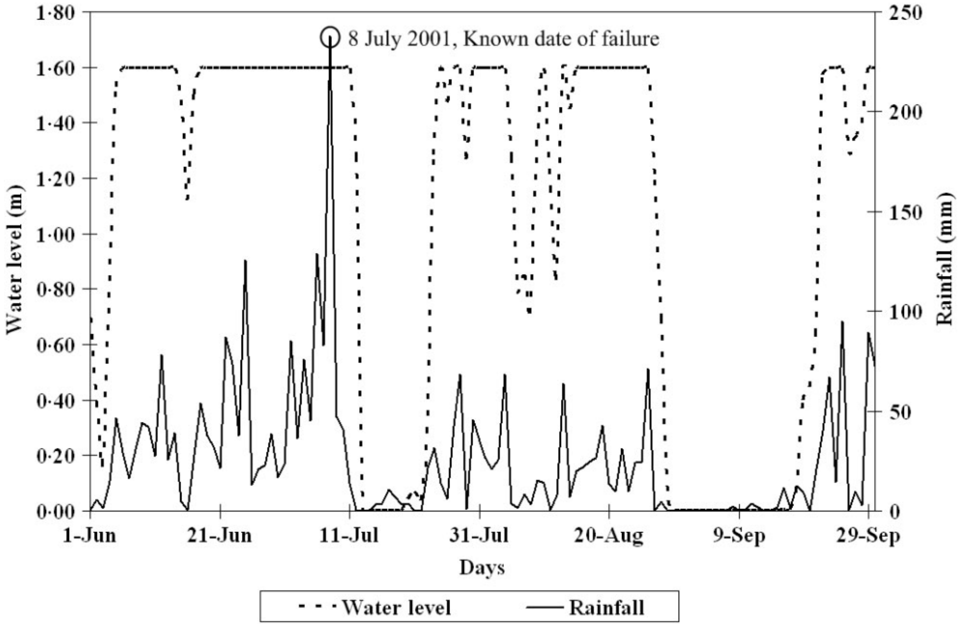


**Figure 8.** Predicted perched water level as a response to rainfall at the location of a shallow landslide during the SW monsoon season of 2001 to 2002.

**Table III.** Average values of the parameters and the sensitivity of the model predictions to root cohesion, soil depth, angle of internal friction and slope at know landslide initiation locations (2000–2001)

| Landslide code | 1 | 2 | 3 | 4 | 5 | 6 | 7 | 8 | 9 | 10 | 11 |
|---|---|---|---|---|---|---|---|---|---|---|---|
| Soil unit | 3 | 3 | 1 | 1 | 1 | 3 | 3 | 3 | 3 | 3 | 3 |
| Land use | R | R | G&R | R | R | FD | FD | G | G | R | G |
| Slope (deg) (Average) | 45·9 | 39·6 | 21·7 | 27·4 | 22·7 | 31·2 | 29·2 | 32·3 | 27·6 | 35·4 | 25·7 |
| Soil thickness (m) (Average) | 0·25 | 0·25 | 1·75 | 1·75 | 3·5 | 1·75 | 0·75 | 0·75 | 0·75 | 1·75 | 0·25 |
| *P*(FOS ≤ 1) | 0·1 | 0·1 | 0·7 | 0·7 | 0·9 | 0·9 | 0·6 | 0·8 | 0·7 | 0·7 | 0·0 |
| *Sensitivity* | | | | | | | | | | | |
| Root cohesion | 0·9 | 0·8 | 0·0 | 0·8 | 0·4 | 0·0 | 0·2 | 0·3 | 0·3 | 0·9 | 0·9 |
| Soil thickness | 0·1 | 0·2 | 0·3 | 0·1 | 0·0 | 0·4 | 0·1 | 0·0 | 0·0 | 0·1 | 0·1 |
| AIF | 0 | 0 | 0·6 | 0·1 | 0·4 | 0·5 | 0·3 | 0·3 | 0·4 | 0·1 | 0·0 |
| Slope | 0·0 | 0·0 | 0·0 | 0·0 | 0·2 | 0·0 | 0·3 | 0·3 | 0·1 | 0·0 | 0·0 |

*Note*: see Tables II and I for parameters linked to soil units and the standard deviation values respectively. R, rubber; G&ER, grassland and rock; FD, forest degraded; G, grassland; *P*(FOS ≤ 1), probability of the Factor of Safety to be less than or equal to one; AIF, angle of internal friction.

predicted as failed demonstrates the capability of the models to be used for susceptibility estimation. The region predicted as unstable (Figure 7a) was also predicted as having a higher average probability of failure (≥50%) compared with the rest of the region (≤2%).

The area susceptible to failure was consistently overestimated when the same inputs were used in SINMAP, SHALSTAB, TRIGERS and STARWARS+PROBSTAB. The prediction of STARWARS+PROBSTAB was marginally better (Kuriakose *et al.*, 2008b). Thus it could be inferred that the errors are a consequence of the poor data quality, especially the digital terrain model (DTM) resolution, overall cohesion and soil depth.

A probabilistic assessment of instability is constrained by the quality of input data and assumed pattern of probability. The FOSM method used for the probability of failure calculations in this study assumes the variability of a parameter as a normal curve. The assumption of a normal curve is not always true, especially for constantly evolving variables such as soil depth. This necessitates a sensitivity analysis. The study was also limited by the fact that the most variable and time dependent parameter, perched water table and volumetric moisture content, was not utilized for assessing the probability of failure.

## Sensitivity of STARWARS

Table IV provides the simulated hydrological effects and transient hydrological conditions of 8 July 2001 at the landslide locations. Though the region has significant vegetation cover interception effect on the day of failure at these locations was negligible. Canopy interception resulted in less than 1% reduction of the rainfall at the landslide locations. This can be attributed to the insignificance of interception in tropical climates (both in absolute and relative terms) as large drop sizes in the rainfall and high throughfall results in reduced interception loss from tropical trees compared with those in temperate climates (Calder, 2001; Jorge and Sharika, 2000).

Evapotranspiration was also insignificant on the day of failure. This corroborates the observations made by researchers (Nizinski *et al.*, 1994; Watanabe *et al.*, 2004; Yusop *et al.*, 2003) that on days of heavy rainfall, evapotranspiration is negligible in



DOI: 10.1002/esp

**Table IV.** Slope hydrology prediction by STARWARS for 8 July 2001 at the landslide initiation locations of 2001, with and without considering the hydrological effects (interception and evapotranspiration) of vegetation

| LC | RF (mm) | $I_c$ (mm) | BT | AET | ERF V (mm) | ERF NV (mm) | WL V (m) | WL NV (m) |
|---|---|---|---|---|---|---|---|---|
| 1 | 237·8 | 2·4 | 0·54 | 0·02 | 236·7 | 237·8 | 0·25 | 0·25 |
| 2 | | 2·3 | 0·54 | 0·05 | 236·7 | | 0·25 | 0·25 |
| 3 | | 0·4 | 0·00 | 0·01 | 237·4 | | 1·75 | 1·75 |
| 4 | | 1·0 | 0·41 | 0·01 | 237·2 | | 1·75 | 1·75 |
| 5 | | 0·9 | 0·00 | 0·01 | 237·9 | | 3·20 | 3·20 |
| 6 | | 1·5 | 0·53 | 0·02 | 237·1 | | 1·75 | 1·75 |
| 7 | | 1·2 | 0·15 | 0·03 | 236·8 | | 0·75 | 0·75 |
| 8 | | 0·6 | 0·00 | 0·01 | 237·2 | | 0·75 | 0·75 |
| 9 | | 0·7 | 0·10 | 0·04 | 237·1 | | 0·75 | 0·7 |
| 10 | | 1·2 | 0·40 | 0·02 | 237·1 | | 1·75 | 1·75 |
| 11 | | 0·6 | 0·00 | 0·03 | 237·2 | | 0·25 | 0·25 |

*Note*: LC, landslide code; RF, rainfall; ERF, effective rainfall; $I_c$, interception; AET, actual evapotranspiration; WL, water level; BT, bulk throughfall ratio; V, considering interception and evapotranspiration; NV, without considering interception and evapotranspiration.

tropical climatic conditions. Although interception and evapotranspiration did not have significant influence in the generation of pore water pressure on the day of failure, they still have relevance in maintaining the long-term non-critical hydrological conditions of the slopes. Considering the fact that the region received at least three days of heavy rainfall prior to the actual day of failure the hydrological effect of vegetation especially evapotranspiration, may be the reason for the delay in the occurrence of landslides (Figure 8).

Sensitivity of the model results to the soil hydrology parameters were not treated independently. Rather, the daily variation of perched water table (Figure 8) can be considered to represent the variability of pore water pressure capable of triggering shallow landslides for the period under consideration.

### Sensitivity of PROBSTAB

PROBSTAB enables sensitivity analysis as an outcome of probability of failure assessment using the FOSM method. The range and standard deviation values of the parameters used for calculating the probability of failure using the FOSM method are provided in Table I. Sensitivity was spatially quantified as a score for each pixel, the contribution of the parameter to the variance of the Factor of Safety at that pixel, using a scale that indicates increasing sensitivity from zero to one. Table III shows the sensitivity of the model results to root cohesion, soil depth, AIF and slope at the known landslide initiation locations.

Sensitivity analysis indicated that the slope stability of the catchment is highly sensitive to root cohesion (Table III and Figure 9). From the comparison of model predictions with and without mechanical effects of vegetation (Figure 7) it could be concluded that inherently unstable slopes planted with rubber are predicted stable primarily as a result of root cohesion. Field observations showed a significant increase in instability when rubber plantations are in their young stage, between one to seven years of planting, though this study did not avail any results to conclusively state so. It must be noted that these conclusions are made ignoring root pullout condition and overestimating root anchorage, thus probably overestimating root cohesion. Well constructed in-sloping terraces also play an important role in ensuring stability, which was also not addressed in the present study.

Variability of soil depth and uncertainty of estimating it in the field makes it a parameter to which the model results were highly sensitive (Table III and Figure 9). Soil depth map used for this research (Figure 4a) had fixed depth values aggregated as polygons, even though inside these polygons slope steepness and consequently soil depth may change considerably. A soil depth map which contains continuous data is expected to be more reliable and should capture varying soil depth in the hollows better. However it is known that evolution of critical soil depth and slope profiles as a consequence of the prevailing rate of weathering are the main preparatory agents for slope failure in soil material (Dykes, 2002). Most models (e.g. TRIGRS, GEOTop-FS, SHETRAN, etc.) including the one used for this study does not address this evolution of the preparatory variables over a long period thus hampering calibration and validation efforts.

Other parameters to which the model results were sensitive are AIF and slope (Figure 9). Model outputs showed little sensitivity to soil cohesion, surcharge and bulk density. Surcharge may have more relevance when wind loading is parameterized and incorporated into the model, which is not the case in the present study. Field evidences and interviews with the local population indicated that debris flows are often initiated during torrential and persistent rainfall associated with high velocity winds.

## Conclusions

Although the study resulted in outputs that have physical meaning the evaluation of the model performance was hampered by the limited nature of the calibration and validation data. Thus the results are merely indicative of the capability that can be achieved by such models in evaluating the spatio-temporal probabilities of landslide initiation.

Despite such limitations, the general temporal pattern of pore water pressure associated to the known period of failure (SW monsoon) was captured by the model (Figure 8). The results indicate that the antecedent moisture conditions and the persistence of high pore water pressure for a significantly long period may have been the immediate preparatory conditions for the failures. The trigger of the events was probably an extremely high intensity rainfall which resulted in a sharp increase of pore water pressure. The model could not predict this sharp response on the actual date of failure probably due to the temporal resolution of the data used. Following the deterministic criteria of $F < 1$, the spatial pattern of instability was overestimated both with (Figure 7a) and without (Figure 7b) accounting the mechanical effects of vegetation. However, the overestimation is comparable with other physically based slope stability assessments (Borga *et al.*, 1998; Simoni *et al.*, 2008; van Beek and van Asch, 2004).

The research conclusively highlights the significance of root cohesion in slope stability assessments. Rubber plantations as they exert considerable root cohesion are good for maintaining the overall stability of the region. However long-term stability is not assured owing to the cropping cycle. It is recommended that along the walls of the in-sloping terraces in the unstable area (Figure 7a), plants that are known to offer significant root cohesion such as Vetiver (*Vetiveria zizanioides*) (The Vetiver Network, 2005) should be planted to ensure stability. Maintaining the hollows devoid of regolith and cleared of obstructions will be an appropriate measure to reduce the spatio-temporal frequency of shallow landslides in



DOI: 10.1002/esp

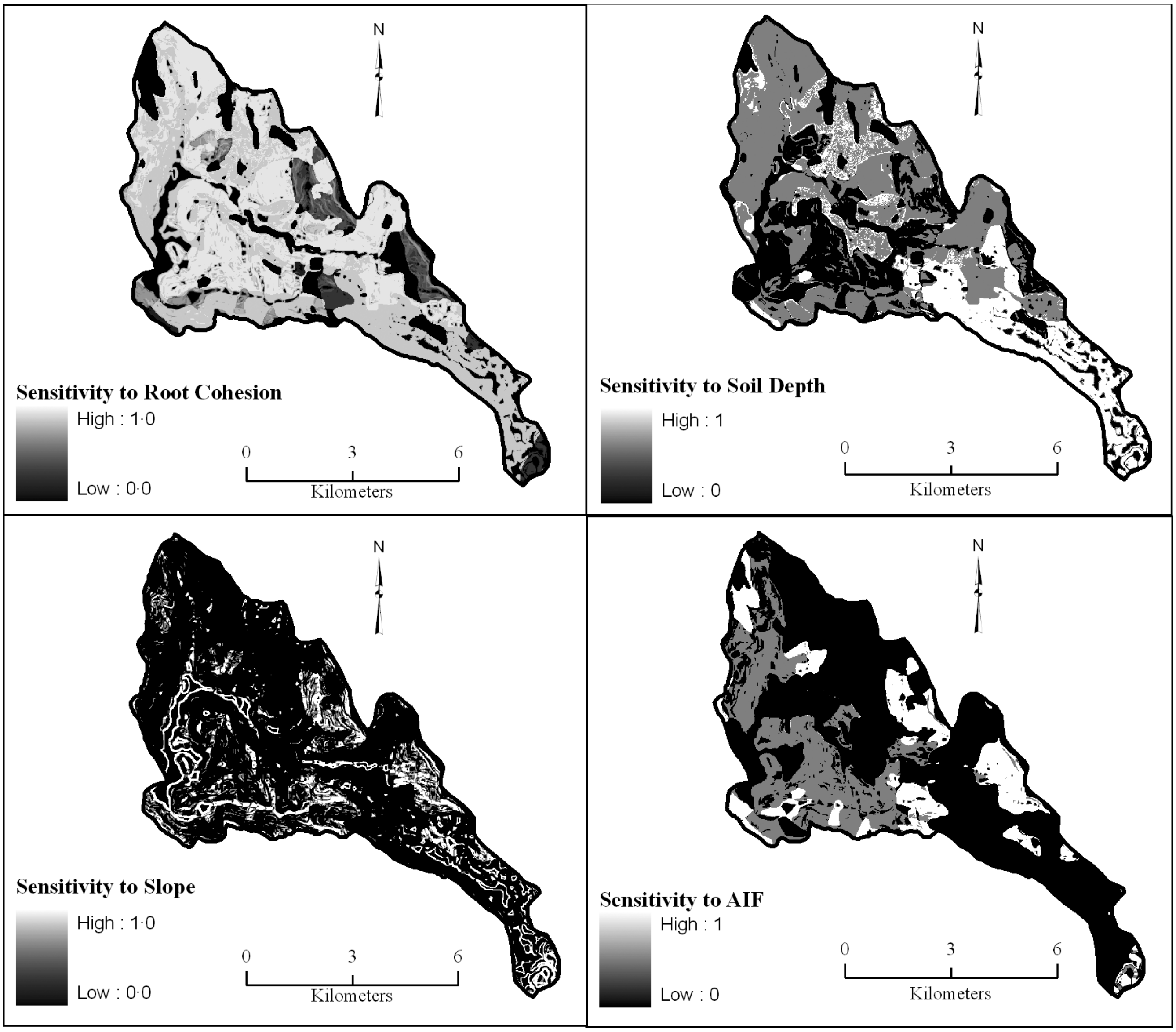


**Figure 9.** A spatial comparison of the sensitivity of slope stability to root cohesion, soil depth, slope and angle of internal friction (sensitivity score for each pixel is the contribution of the parameter to the variance of the Factor of Safety at that pixel represented using a scale that indicates increasing sensitivity from zero to one. It is unit less).

the region. The effect of terracing, uprooting, planting pits and the macropores as a result of root decay on slope hydrology and slope stability of the region necessitates further enquiry.

Sensitivity analysis shows that with better DTM, land-use/land-cover maps, topographical and pedological parameters, prediction of the spatio-temporal probabilities of landslides in the region using physically based models can be significantly improved. An accurate spatial estimate of soil depth needs to be the priority of researchers in the parameterization of a physically based slope hydrology-slope stability model.

The ongoing trend towards quantitative assessments in geomorphology stimulates the application of physically based models for evaluating earth surface processes such as landslides even in data deficient countries. In light of this research it could be concluded that such complex models when used in a data poor setting, though may not assure reliable landslide hazard quantification, are suitable for quantitatively assessing the influence of various parameters contributing to slope stability.

*Acknowledgements*—The researchers acknowledge the contributions made by Professor R.C Lakhera, Scientist, Indian Institute of Remote Sensing (IIRS), Dehradun, and Mr G. Sankar, Scientist, Centre for Earth Science Studies (CESS), Thiruvananthapuram, India, towards successfully completing this study. We also thank, Dr Dinand Alkema, Lecturer, ITC and Dr T.W.J van Asch, Lecturer (Rtd.), Utrecht University for their guidance and constant help. Thanks are due to Dr V. Hari Prasad, Scientist, IIRS, for his constant support. We thank Dr V.K Dadhwal, Dean, IIRS and Dr M. Baba, Director, CESS for their support in successfully completing this research. We also thank the extreme patience and efforts of the reviewers for helping us improve the article to its present form.

## References

Ang AH-S, Tang WH. 1984. *Probability Concepts in Engineering Planning and Design: Decision, Risk, and Reliability, II*. Wiley: New York.

Aston AR. 1979. Rainfall interception by eight small trees. *Journal of Hydrology* **42**(3–4): 383–396.

Barredo J, Benavides A, Hervas J, van Westen CJ. 2000. Comparing heuristic landslide hazard assessment techniques using GIS in the Tirajana basin, Gran Canaria Island, Spain. *International Journal of Applied Earth Observation and Geoinformation* **2**(1): 9–23.

Basak P, Narasimha Prasad NB. 1989. Recurring landslides in the

Western Ghats – an environmental hazard. *Environmental Conservation* **16**(2): 169–172.

Bathurst JC, Moretti G, El-Hames A, Begueria S, Garcia-Ruiz JM. 2007. Modelling the impact of forest loss on shallow landslide sediment yield, Ijuez river catchment, Spanish Pyrenees. *Hydrology and Earth Systems Sciences* **11**(1): 569–583.

Baum RL, Savage WZ, Godt JW. 2002. *TRIGRS – A Fortran Program for Transient Rainfall Infiltration and Grid Based Regional Slope Stability Analysis*, Open file report 02-424. US Department of the Interior and US Geological Survey: Denver, CO.

Borga M, Dalla Fontana G, Da Ros D, Marchi L. 1998. Shallow landslide hazard assessment using a physically based model and digital elevation data. *Environmental Geology* **35**(2): 81–88.

Calder I. 2001. Canopy processes: implications for transpiration, interception and splash induced erosion, ultimately for forest management and water resources. *Plant Ecology* **153**(1–2): 203–214.

Castellanos Abella EA, van Westen CJ. 2007. Generation of a landslide risk index map for Cuba using spatial multi-criteria evaluation. *Landslides* **4**(4): 311–325.

Census of India. 2001. *Population Distribution, Percentage Decadal Growth Rate, Sex Ratio and Population Density of Kerala, 2001*. Government of India: Thiruvananthapuram, Kerala.

Chandrakaran S, Paul KV, Nambiar MRM. 1995. *Geotechnical Characteristics of Landslide Prone Areas of Idukki and Kottayam Districts of Kerala*, Abstracts of the National Seminar on Landslides in Western Ghats, 29–30 August. Centre for Earth Science Studies, Government of Kerala: Thiruvananthapuram.

Dietrich WE, Montgomery DR. 1998. *SHALSTAB: A Digital Terrain Model for Mapping Shallow Landslide Potential*. University of California and University of Washington: Berkeley, CA.

Doorenbos J, Pruitt WO. 1977. *Crop Water Requirements*, Irrigation and Drainage Paper 24. Food and Agriculture Organization of the United Nations: Rome.

Dykes AP. 2002. Weathering-limited rainfall-triggered shallow mass movements in undisturbed steepland tropical rainforest. *Geomorphology* **46**(1–2): 73–93.

Ewen J, Parkin G, O'Connell PE. 2000. SHETRAN: distributed river basin flow and transport modeling system. *Journal of Hydrologic Engineering* **5**(3): 250–258.

Farrel D, Larson W. 1972. Modelling the pore structure of porous media. *Water Resources Research* **8**: 699–705.

Fasullo J, Webster PJ. 2002. A hydrological definition of Indian monsoon onset and withdrawal. *Journal of Climate* **16**(19): 3200–3211.

Fredlund DG. 1987. Slope stability analysis incorporating the effect of soil suction. In *Slope Stability: Geotechnical Engineering and Geomorphology*, Anderson MG, Richards KS (eds). John Wiley & Sons: Chichester; 113–144.

George PS, Chattopadhyay S. 2001. Population and land use in Kerala. In *Growing Populations Changing Landscapes: Studies from India, China, and the United States*, Wolman MG (ed.). National Academy Press: Washington, DC; 79–106.

Glade T. 2003. Landslide occurrence as a response to landuse change: a review of evidence from New Zealand. *CATENA* **51**(3–4): 297–314.

Glickman TS (ed.). 2000. *Glossary of Meteorology*. American Meteorological Society and Allen Press: Cambridge.

Gopinath CI. 1985. *Debris Flows in the Western Ghats* [*Urulpottal Paschimaghattathil* (in Malayalam)], Workshop on Landslides in Western Ghats, 30–31 July. Kerala State Committee on Science, Technology and Environment, Kozhikode.

Gorsevski PV, Gessler PE, Boll J, Elliot WJ, Foltz RB. 2006. Spatially and temporally distributed modelling of landslide susceptibility. *Geomorphology* **80**(3–4): 178–198.

Greenway DR. 1987. Vegetation and slope stability. In *Slope Stability*, Gerson M, Richards KS (eds). John Wiley & Sons: Chichester; chapter 6.

Guzzetti F, Reichenbach P, Cardinali M, Galli M, Ardizzone F. 2005. Probabilistic landslide hazard assessment at the basin scale. *Geomorphology* **72**(1–4): 272–299.

Hargreaves GH, Samani ZA. 1982. Estimating potential evapotranspiration. *Journal of Irrigation and Drainage Engineering* **108**(IR3): 223–230.

Harikrishnan K *et al*. 1995. *Proper Landuse Practice – An Effective Mitigation Measure for Landslide*, Abstracts of the National Seminar on Landslides in Western Ghats, 29–30 August. Centre for Earth Science Studies, Government of Kerala: Thiruvananthapuram.

Immerzeel WW, Gaur A, Zwart SJ. 2008. Integrating remote sensing and a process-based hydrological model to evaluate water use and productivity in a south Indian catchment. *Agricultural Water Management* **95**(1): 11–24.

James EJ, Pradeepkumar PK, Rangana G, Nayak IV, Ravi TB. 1981. *Studies on the Hydrological Processes in the Forest Drainage Basins of the Western Ghats of India*, International symposium on Forest Hydrology and Watershed Management, Vancouver, Canada. International Association of Hydrological Sciences, Publication No. 167. International Association of Hydrological Sciences: Wallingford; 223–229.

Jorge AR, Sharika S. 2000. A statistical-dynamical parameterization of interception and land surface-atmosphere interactions. *Journal of Climate* **13**(22): 4050–4063.

Karssenberg D. 2002. *Building Dynamic Spatial Environmental Models*. PhD Thesis, Utrecht University; 222 pp.

Kuriakose SL, Lele NV, Joshi PK. 2006. *Fractional Vegetation Cover Estimation from MODIS NDVI Data – A Comparison of Methods and Application in Dynamic Numerical Modelling for Debris Flow (Urul Pottal) Initiation Prediction*, International conference on Natural Hazards and Disasters – Local to Global Perspectives, 25–27 November, Anantapur, India. IGS Conference Publication (CDRom), Sri Krishnadevaraya University and the Indian Geographical Society: Anantapur.

Kuriakose SL, Sankar G, Muraleedharan C. 2008a. History of landslide susceptibility and a chorology of landslide prone areas in the Western Ghats of Kerala, India. *Environmental Geology*. DOI: 10.1007/s00254-008-1431-9

Kuriakose SL, van Beek LPH, van Westen CJ. 2008b. *Comparison of Physically Based Models for Debris Flow Initiation – A Case Study in the Tikovil River Basin of the Western Ghats of Kerala, India*, European Geosciences Union General Assembly 2008, Vienna, Austria. http://www.cosis.net/abstracts/EGU2008/01548/EGU2008-A-01548.pdf. Geophysical Research Abstracts, Vol 10 (EGU2008-A-01548).

Kutılek M, Nielsen DR. 1994. *Soil Hydrology*. Catena-Verlag: Cremlingen-Destedt; 370 pp.

Langsholt E. 1992. A water balance study in lateritic terrain. *Hydrological Processes* **6**: 11–17.

Malet J-P, van Asch TWJ, van Beek LPH, Maquaire O. 2005. Forecasting the behaviour of complex landslides with a spatially distributed hydrological model. *Natural Hazards and Earth System Sciences* **5**: 71–85.

Millington RJ, Quirk JP. 1959. Permeability of porous media. *Nature* **183**: 387–388.

Murali Kumar B. 2007. *Flood Situation Report – 2007* (No. 137/2007, 1700 hours, LAST SITREP). Disaster Management Division, Ministry of Home Affairs, Government of India: New Delhi.

National Bureau of Soil Survey (NBSS) and Landuse Planning (LUP). 1999. *Resource Soil Survey and Mapping of Rubber Growing Soils of Kerala and Tamil Nadu on 1:50 000 scale – Consultancy Project for Rubber Research Institute of India, Kottayam*. NBSS and LUP: Nagpur.

Nilaweera NS, Nutalaya P. 1999. Role of tree roots in slope stabilisation. *Bulletin of Engineering Geology and Environment* **57**(4): 337–342.

Nizinski J, Morand D, Fournier C. 1994. Actual evapotranspiration of a thorn scrub with Acacia *tortilis* and Balanites *aegyptiaca* (North Senegal). *Agricultural and Forest Meteorology* **72**(1–2): 93–111.

Pack RT, Tarboton DG, Goodwin CN. 1998. *The SINMAP Approach to Terrain Stability Mapping*, eighth congress of the International Association of Engineering Geology, Vancouver, British Columbia, Canada. International Association of Engineering: Paris.

Penman HL. 1948. Natural evaporation from open water, bare soil and grass. *Proceedings of the Royal Society of London* **A**(194): S120–S145.

Refsgaard JC *et al*. 1992. Application of the SHE to catchments in India Part 1: general results. *Journal of Hydrology* **140**(1–4): 1–23.

Roering JJ, Schmidt KM, Stock JD, Dietrich WE, Montgomery DR. 2003. Shallow landsliding, root reinforcement, and the spatial distribution of trees in the Oregon Coast Range. *Canadian Geotechnical Journal* **40**: 237–253.

Sankar G. 2007. Landslides. In *State of the Environment Report of Kerala 2007 – Volume II: Natural Hazards*, Yesodharan EP, Kokkal K, Harinarayanan P (eds). Kerala State Council for Science, Technology and Environment, Government of Kerala: Thiruvananthapuram; 116–156.

Santacana N, Baeza B, Corominas J, de Paz A, Marturia J. 2003. A GIS-based multivariate statistical analysis for shallow landslide susceptibility mapping in La Pobla de Lillet area (Eastern Pyrenees, Spain). *Natural Hazards* **30**: 281–295.

Schaap MG. 1999. *Rosetta Manual*. US Salinity Laboratory: Riverside, CA.

Schaap MG, Leij FJ, van Genuchten MT. 2001. ROSETTA: a computer program for estimating soil hydaulic parameters with hierarchical pedotransfer functions. *Journal of Hydrology* **251**: 163–176.

Schmidt RL *et al*. 2001. The variability of root cohesion as an influence on shallow landslide susceptability in the Oregon Coast Range. *Canadian Geotechnical Journal* **35**(5): 995–1024.

Simoni S, Zanotti F, Bertoldi G, Rigon R. 2008. Modelling the probability of occurrence of shallow landslides and channelized debris flows using GEOtop-FS. *Hydrological Processes* **22**(4): 532–545.

Singh R, Tiwari KN, Mal BC. 2006. Hydrological studies for small watershed in India using the ANSWERS model. *Journal of Hydrology* **318**(1–4): 184–199.

Skempton AW, DeLory FA. 1957. *Stability of Natural Slopes in London Clay*, Fourth International Conference on Soil Mechanics and Foundation Engineering, London.

Soman K. 2002. *Geology of Kerala*. Geological Society of India: Bangalore.

Souvenir Committee. 1982. *Adukkom Sabha Centenary Souvenir*. St Pauls C.S.I Church Adukkom: Irattupetta; 97 pp.

Spate OHK, Learmonth ATA, Farmer BH, Learmonth AM. 1967. *India, Pakistan and Ceylon: The Regions*. Methuen and Co Ltd: London.

Srinivasan K, Kunhamu TK, Mohankumar B. 2004. Root excavation studies in a mature rubber plantation. *Natural Rubber Research* **17**(1): 18–22.

Styczen ME, Morgan RPC. 1995. Engineering properties of vegetation. In *Slope Stabilization and Erosion Control: A Bioengineering Approach*, Morgan RPC, Rickson RJ (eds). E&FN Spon: London.

Thakur VC. 1996. *Landslide Hazard Management and Control in India*, Status Report. International Center for Integrated Mountain Development: Kathmandu, Nepal.

Thampi PK, Mathai J, Sankar G, Sidharthan S. 1998. *Evaluation study in terms of landslide mitigation in parts of Western Ghats, Kerala*, Research report submitted to the Ministry of Agriculture, Government of India. Centre for Earth Science Studies, Government of Kerala: Thiruvananthapuram.

The Vetiver Network. 2005. *Introduction to Vetiver Network*. The Vetiver Network: Bellingham, WA.

van Beek LPH. 2002. *Assessment of the Influence of Changes in Landuse and Climate on Landslide Activity in a Mediterranean Environment*. PhD Thesis, University of Utrecht; 363 pp.

van Beek LPH, van Asch TWJ. 2004. Regional assessment of the effects of land-use change and landslide hazard by means of physically based modelling. *Natural Hazards* **30**(3): 289–304.

van Genuchten MT. 1980. A closed form equation for predicting the hydraulic conductivity of unsaturated soils. *Soil Science Society of America Journal* **44**: 892–898.

van Westen CJ, Castellanos Abella EA, Kuriakose SL. 2008. Spatial data for landslide susceptibility, hazard and vulnerability assessment: an overview. *Engineering Geology* **102**(3–4): 112–131.

van Westen CJ, van Asch TWJ, Soeters R. 2005. Landslide hazard and risk zonation: why is it still so difficult? *Bulletin of Engineering Geology and Environment* **65**(2): 167–184.

Varnes DJ and IAEG Commission on Landslides and other Mass-Movements. 1984. *Landslide Hazard Zonation: Review of Principles and Practice*. UNESCO: Paris.

Victor OCD. 1962. *Kurisumala: A Socio-economic Survey*. St Joseph's Apostolic Seminary: Alwaye, India; 87.

Von Hoyningen-Huene J. 1981. *Die Interzeption Des Niederschlags in landwirtschaftlichen Pflanzenbeständen*. Arbeitsbericht DeutscherVerband fürWasserwirtschaft und Kulturbau, DVWK: Brunswick.

Waldron LJ. 1977. The shear resistance of root-permeated homogenous and stratified soil. *Soil Science Society of America Journal* **41**: 843–849.

Walthall C *et al*. 2004. A comparison of empirical and neural network approaches for estimating corn and soybean leaf area index from Landsat ETM+ imagery. *Remote Sensing of Environment* **92**(4): 465–474.

Watanabe K *et al*. 2004. Changes in seasonal evapotranspiration, soil water content and crop coefficients in sugarcane, cassava and maize fields in northeast Thailand. *Agricultural Water Management* **67**(2): 133–143.

Wilkinson PL, Anderson MG, Lloyd DM, Renaud J-P. 2002. Landslide hazard and bioengineering: towards providing improved decision support through integrated numerical model development. *Environmental Modelling and Software* **17**(4): 333–344.

Wu TH, McKinnell WPI, Swanston DN. 1979. Strength of tree roots and landslides on Prince of Wales Island, Alaska. *Canadian Geotechnical Journal* **16**: 19–33.

Yusop Z, Yen CS, Hui CJ. 2003. Throughfall, stemflow and interception loss of old rubber trees. *Jurnal Kejuruteraan Awam* **15**(1): 24–33.

Ziemer RR. 1981. *Roots and the Stability of Forested Slopes*, International Symposium on Erosion and sediment transport in Pacific Rim Steeplands, 25–31 January, Christchurch, New Zealand, International Association of Hydrological Sciences, Publication No. 132. International Association of Hydrological Sciences: Wallingford; 343–361.